

Stochastic oscillations in Josephson tunnel junctions

V. N. Gubankov, S. L. Ziglin, K. I. Konstantinyan, V. P. Koshelets, and G. A. Ovsyannikov

Institute of Radio Engineering and Electronics, USSR Academy of Sciences

(Submitted 6 June 1983)

Zh. Eksp. Teor. Fiz. **86**, 343–351 (January 1984)

The dynamics of the onset of stochastic oscillations in Josephson tunnel junctions is investigated in a wide range of external microwave fields. The experimental data are compared with analytic and numerical calculations of the conditions of the formation of stochastic oscillations. The calculations are carried out within the framework of the resistive model of the Josephson junction.

1. INTRODUCTION

Much attention is being paid in the past few years to nonlinear dynamic systems in which stochastic oscillations (SO) of high intensity can be caused by the appearance of complicated trajectories—strange attractors—in phase space (see, e.g., Refs. 1 and 2). These oscillations have a broad spectrum and are practically indistinguishable from fluctuations of the system.

Stochastic oscillations produced in Josephson tunnel junctions by the action of an external microwave signal were analyzed in Refs. 2–8. Their spectrum and the ranges of variation of the junction parameters, as well as the characteristics of the microwave action under which stochastic oscillations take place, were determined by numerical calculations and by analog simulation. No analytic expressions, however, were obtained for the conditions under which the stochastic oscillations set in.

In a preceding paper⁹ we reported experimental observation of stochastic oscillations in Josephson tunnel junctions, although without a detailed analysis of the conditions for the onset of these oscillations. In the present paper we report the results of an experimental and theoretical investigation of stochastic oscillations in such junctions and compare the experimentally observed regions where these oscillations appear with the results of the analytic and numerical methods.

2. THEORY

In calculations of the processes that give rise to stochastic oscillations in Josephson tunnel junctions it is customary to use^{3–8} a resistive model,¹⁰ according to which the current through the junction can be represented as a sum of the currents $I_c \sin \varphi$ through an ideal Josephson junction, and also in terms of its normal resistance, V/R_N , and the capacitance Cd^2V/dt^2 (I_c is the critical current and V is the voltage across the junction). Using the customary normalization for Josephson junctions, the equation for the phase difference φ at an external-microwave frequency f_e takes the form

$$\ddot{\varphi} + \beta^{-1/2} \dot{\varphi} + \sin \varphi = i_0 + i_1 \sin z, \quad (1)$$

Here $\beta = 2eI_c R_N C / \hbar$ is a parameter indicative of the damping of the plasma oscillations in the junction, $i_0 = I_0/I_c$, and $i_1 = I_1/I_c$, where I_0 is the direct current through the junction and I_1 is the microwave current amplitude; $\omega = f_e/f_p$,

where $f_p = (2\pi)^{-1}(2eI_c)/\hbar c)^{1/2}$. The time is measured in units of $(2\pi f_p)^{-1}$.

2.1. Separatrices of the system

For future convenience, we rewrite (1) in the form of a system of first-order equations:

$$\begin{aligned} \dot{\varphi} &= v, \\ \dot{v} &= -\sin \varphi - \beta^{-1/2} v + i_0 + i_1 \sin z, \quad \dot{z} = \omega. \end{aligned} \quad (2)$$

At $\beta^{-1/2} = i_0 = i_1 = 0$ the system (2) describes autonomous oscillations of a physical pendulum in a gravitational field. The phase portrait of these oscillations is well known (see, e.g., Ref. 11). In view of the cylindrical symmetry of the system it is convenient to choose the phase plane to be the developed surface of a cylinder ($-\pi < \varphi < \pi$), on which there is one stable point (a center with coordinates $\theta_0(0,0)$) and two hyperbolic points (saddles $\theta_{1,-1}(0, \pm\pi)$, Fig. 1). The saddles are joined by separatrices (dashed lines in Fig. 1), which are described by the equations

$$v = \pm 2 \cos(\varphi/2). \quad (3)$$

At $i_1 \neq 0$ the phase trajectories of the system (2) depend also on a third coordinate z . To analyze the phase portrait of the system (2) in this case one can use the mapping of the plane $z = \text{const}$ over the period of the external action. At small perturbations ($\beta^{-1/2} = i_0, i_1 \ll 1$) this mapping has immobile hyperbolic points close to the points $\theta_{1,-1}$, the stable and unstable manifolds¹⁾ of which differ little from the unperturbed separatrices.

According to the results of symbolic dynamics (see, e.g.,

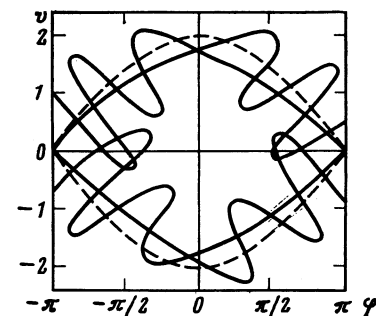


FIG. 1. Separatrices of the system (2). Dashed—unperturbed separatrices, solid—mapping of stable and unstable manifolds of the points $\theta_{1,-1}$ at $i_1 \neq 0$.

Ref. 12) the sufficient condition for the onset of stochastic oscillations in a perturbed system is an intersection of the stable and unstable manifolds of the perturbed points $\theta_{1,-1}$ at nonzero angle (see Fig. 1). Since the unperturbed system has a first integral

$$H = \frac{1}{2}v^2 - \cos \varphi, \quad (4)$$

a sufficient condition for the intersection of the corresponding stable and unstable manifolds of the points θ_1 and θ_{-1} is according to Ref. 13 the possession of a simple zero by the function

$$J(\tau) = \int_{-\infty}^{\infty} \dot{H}(v^{(a)}(t), \varphi^{(a)}(t), t+\tau) dt, \quad (5)$$

where \dot{H} is the derivative of H with respect to t along the solution of the perturbed system, and $\varphi^{(a)}(t), v^{(a)}(t)$ are the unperturbed asymptotic solutions that pass through the hyperbolic points θ_1 and θ_{-1} (dashed in Fig. 1):

$$\varphi^{(a)} = -\pi + 4 \operatorname{arctg}(\pm t), \quad v^{(a)} = \pm 2 \operatorname{ch}^{-1} t. \quad (6)$$

Substituting (6) in the expression for $J(\tau)$ and integrating, we obtain

$$J(\tau) = 8\beta^{-1/2} \pm 2\pi i_0 + 2\pi i_1 \operatorname{ch}^{-1}(\pi\omega/2) \sin \omega\tau. \quad (7)$$

Consequently $J(\tau)$ has a simple zero if the condition

$$|-4/\pi\beta^{1/2} \pm i_0| < i_1 \operatorname{ch}^{-1}(\pi\omega/2) \quad (8)$$

is satisfied; this is the sought condition for the onset of stochastic oscillations in the system (2).²⁾ The reversal of the sign of i_0 corresponds to a different direction of dc current flow through the junction, so that in the presence of i_0 the system goes over into the stochastic-oscillation regime at lower values of i_1 .

Relation (8) can be easily generalized to the case when a tunnel junction is connected in a superconducting ring with inductance L (high-frequency superconducting quantum interference device—HF SQUID). Equation (1) acquires an additional term φ/l ($l = 2\pi LI_c / \Phi_0$, $\Phi_0 = h/2e$ is the magnetic-flux quantum) due to the presence of magnetic flux in the ring. Proceeding in analogy with the case considered above, we obtain at $l \gg 1$ the condition for the onset of stochastic oscillations:

$$|-4/\pi\beta^{1/2} \pm i_0 + 2\pi m/l| < i_1 \operatorname{ch}^{-1}(\pi\omega/2), \quad (9)$$

where $m = 0, \pm 1, \pm 2, \dots$ characterizes the number and direction of the quanta of the flux Φ_0 which are contained in the ring.

2.2. Kolmogorov's entropy

The analytic expressions obtained for the regions where stochastic oscillations occur are valid when the system is close to conservative. To determine the limits of these regions under strong perturbations we have carried out a numerical calculation, and considered the following circumstance. It is known that for a strange attractor to appear all the trajectories must enter into a certain region and at the same time diverge in the interior of this region.¹

For the system of equations (2) the first condition is certainly satisfied at all values of the parameters, since contraction of the phase space takes place:

$$\frac{\partial \dot{\varphi}}{\partial \varphi} + \frac{\partial \dot{v}}{\partial v} + \frac{\partial \dot{z}}{\partial z} = -\frac{1}{\beta^{1/2}} < 0. \quad (10)$$

The criterion for the divergence of the phase trajectories was chosen to be positiveness of the Kolmogorov entropy,¹⁵ defined as follows:

$$K = \lim_{\tau \rightarrow \infty} k(\tau), \quad k(\tau) = \frac{1}{\tau} \frac{D(\tau)}{D(0)}, \quad (11)$$

$$D(\tau) = [(\varphi_1 - \varphi_2)^2 + (v_1 - v_2)^2]^{1/2},$$

where $D(\tau)$ is the distance, at the instant τ , between two phase points (φ_1, v_1) and (φ_2, v_2) that were separated at the instant $\tau = 0$ by a distance $D(0)$. If the motion of the system is stochastic, the distance between the phase trajectories increases exponentially with time ($K > 0$). In the opposite case ($K < 0$) the trajectories go off to a stable limit cycle as $t \rightarrow \infty$.

To calculate K , the system (2) was integrated by the fourth-order Runge-Kutta method. The integration interval was $1/64$ of the period T of the external action. At arbitrary initial conditions, the system (2) was integrated to $t_1 = 30T$, when the settling process already terminated, at least for the region of the regular oscillations. At that instant a small perturbation of the coordinates φ and v was specified, such that $D(0) = 10^{-3}$, after which the calculation was continued for two trajectories (perturbed and unperturbed), and $D(\tau)$ and $k(\tau)$ were determined. In the calculation of k we did not regard as identical the phases φ that differed by an integer times of 2π , to avoid the difficulties connected with the fact that the distance between those points that do not go off to infinity cannot increase without limit.¹⁵

Figure 2 shows the dependence of k on the number N of the oscillation periods of the external action, for three initial conditions: $\varphi(0), v(0)$, and $i_1 = 0.8$, with the remaining parameters fixed at $\omega = 0.52, \beta = 0.25$, and $i_0 = 0$. It can be seen that in the range of large N the value of k depends little on N and at arbitrary initial conditions $k(N)$ tends to a positive limit k with increasing N , the obtained value of K being also independent of the specified perturbation $D(0)$. This means that the distance $D(\tau)$ between the initially close

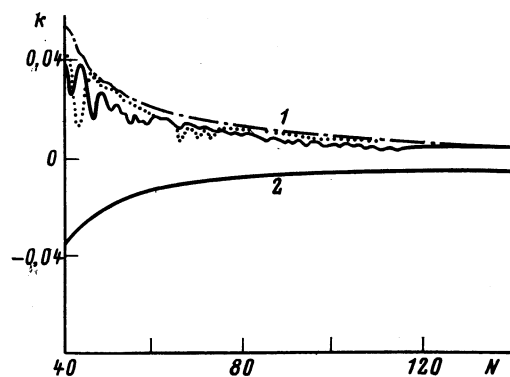


FIG. 2. Dependence of the characteristic exponent k on the number N of periods of the external signal for a junction with $\beta = 25, i_0 = 0, \omega = 52, D(0) = 10^{-3}$ at two external signal amplitudes: 1) $i_1 = 0.8$ for initial conditions $v(0) = 0$ and $\varphi(0) = 0$ (dash-dot curve) $v(0) = 10$ and $\varphi(0) = 10$ (solid curve), $v(0) = -10$ and $\varphi(0) = -10$ (dotted); 2) $i_1 = 0.4$ for all initial conditions.

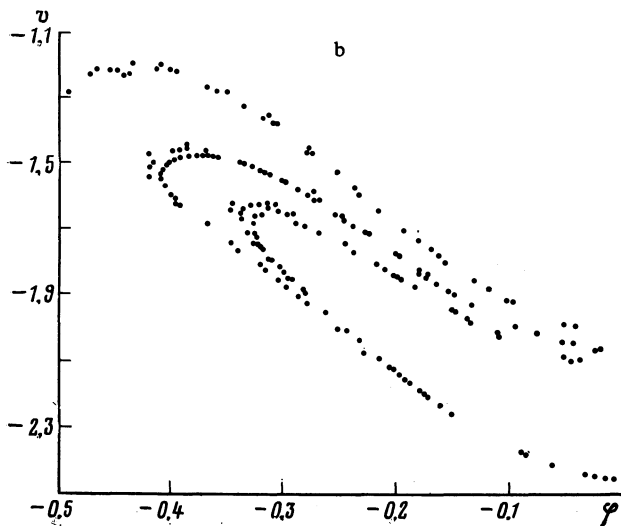
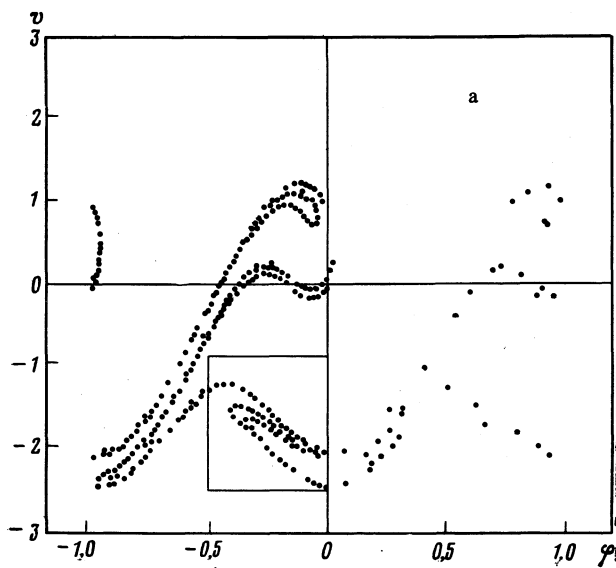


FIG. 3. a) Structure of shift mapping at $i_1 = 0.8$, $i_0 = 0$, $\beta = 0.25$, and $\omega = 0.52$; b) fragment of mapping shown framed in Fig. 3a.

points increases exponentially with time. Figure 2 shows also the $k(N)$ dependence for $i_1 = 0.4$ when there were no stochastic oscillations in the system (2). It can be seen that in this case $k(N) < 0$.

The Kolmogorov entropy was used by us to determine the regions where stochastic oscillations set in. At a fixed frequency ω of the external action the value of i_1 was in-

creased from zero, and at each i_1 step we determined the value of k at $N \sim 100 T$. The appearance of a positive sign of K was evidence of the onset of stochastic oscillations.

To confirm this, we analyzed in the region $K > 0$ the phase trajectories of the system, using the shift mapping.¹¹ We analyzed the coordinates of the points on the $[\varphi, v]$ plane for each period of the external action. Figure 3a shows the shift mapping of the phase trajectories of the system (2) at $i_1 = 0.8$, $i_0 = 0$, $\beta = 25$, and $\omega = 0.52$ for a realization consisting of $10^3 T$ points. It can be seen that many oscillations exist in the systems (harmonics and subharmonics of the external signal), each characterized by a separate point. These points do not lie on a line, but occupy a certain band, thus attesting to the onset of a strange attractor¹ in the system (2). Local analysis of the shift mapping shows that the set of points in the cross section $v = \text{const}$ corresponds to a Cantor set, which is a feature of the strange attractor (Fig. 3b). We note that in a wide range of variation of the parameter $\beta > 25$ the structure of the strange attractor changes little within the region where the stochastic oscillations appear.

3. EXPERIMENT

3.1. Investigated samples and experimental technique

As shown by the theoretical analysis, stochastic oscillations should manifest themselves most strongly for transitions with high values of the parameter β in response to microwaves of frequency close to the plasma frequency f_p . When microwave signals in the millimeter band are used, these conditions are satisfied by Josephson tunnel junctions of the Nb — Nb_xO_y — PbBi type manufactured by the procedure described in Ref. 16. The parameters of the investigated junctions are listed in Table I. The linear dimension of the junction (plan view) is much smaller than the characteristic depth of penetration of the magnetic field, so that uniformity of the current distribution over the entire junction area S is assured. This was tentatively confirmed in Ref. 16 by the dependence of the critical current I_c on the external magnetic field, so that the coordinate dependence of the phase difference φ could be neglected. The value of I_c and the normal resistance R_N of the junction were determined from the current-voltage characteristic (CVC) of the junction measured with direct current. The junction capacitance was calculated from the formula $C = \epsilon S / 4\pi d$ using the following empirical relation¹⁷ for the thickness d of the oxide layer of tunnel junctions based on niobium:

$$\frac{d}{\epsilon} [\text{\AA}] = 1.4 - 0.25 \lg j_{ap} \left[\frac{\text{A}}{\text{cm}^2} \right], \quad (12)$$

TABLE I.

Junction no.	Critical current I_c , μA	Normal resistance R_N , Ω	Area S , μm^2	Capacitance C , pF	The parameter β	Plasma frequency f , GHz
1	440	1.3	19	3.2	7	103
2	32	8.1	21	2.2	14	35
3	115	4.6	38	5.1	40	37
4	225	6.2	14	2.2	56	90
5	522	1	13	2.3	4	132
6	30	18	11	1.6	48	38

with the current density j_{qp} determined from the current jump on the quasiparticle branch of the CVC. The values of f_p and β were calculated using the equations given in Sec. 2 above.

The samples investigated were placed transverse to a flattened ($h = 0.6$ mm) 8-mm-band waveguide equipped with a short-circuiting piston and a post. With microwave radiation of frequency $f_e = 20\text{--}80$ GHz applied, we measured simultaneously the CVC and the junction voltage in one of the following frequency bands: a) $F_1 = 100$ Hz–100 kHz with controllable band $\Delta F_1 = 1\%$, 10% , and 100% of F_1 ; b) $F_2 = 47$ MHz with band $\Delta F_2 = 45$ MHz; c) $F_3 = 470$ MHz with $\Delta F_3 = 450$ MHz. In addition we plotted the time dependences of the junction voltage U in the absence of dc through the junction.

3.2. Experimental results and their discussion

Figure 4 shows the $U(t)$ plots obtained for junction No. 6 at different external-microwave radiation levels at a frequency $f_e = 52.6$ GHz and at $I_0 = 0$. It can be seen that at certain microwave power levels P_e the value of U exceeds that corresponding to the noise of the measuring amplifier ($P_e = 0$). This increase of U is observed in all the bands of the frequency F , thus indicating that the signal U is broadband at least in the frequency range $F = 0$ to 500 MHz. The appearance of such a signal could be due to the presence of Josephson generation, which also has a broad spectrum. In our case, however, there was no dc voltage across the junction ($V = 0$), and consequently no Josephson generation took place. Nor does usual detection of a microwave signal with finite spectral width take place here, in view of the symmetry of the junction CVC.¹⁶ At the same time, according to calculations,⁴ the stochastic oscillations in Josephson tunnel junctions have a very broad spectrum from low frequencies to f_e , so that the observed increases of the alternating voltage U can be identified with the stochastic oscillations. Favoring the last statement is also the fact that, in accord with the calculation,⁴ a nonmonotonic change of U was observed when P_e was varied, but for a junction with a low value of the parameter $\beta \lesssim 15$ the nonmonotonicity led to an alternation of re-

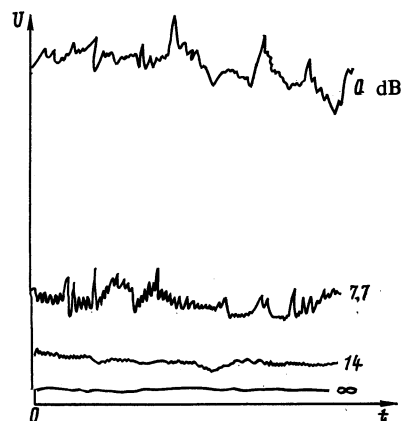


FIG. 4. Dependences of $U(t)$ for junction No. 6 at $\omega = 0.84$, $i_0 = 0$, $\beta = 34$, and $F = F_2$ for different levels of damping introduced in the channel.

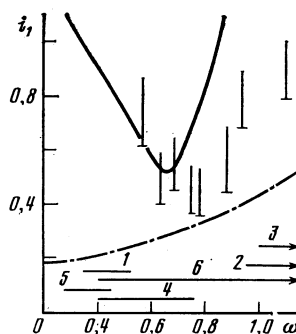


FIG. 5. Horizontal segments—experimental bands of frequency in which stochastic oscillations were observed for the junctions listed in the table. The upper frequency limit for the observation of stochastic oscillations for junctions 2, 3, and 6 reached ≈ 1.5 . Vertical segments—lower amplitude limits of the stochastic oscillations for junction No. 6 at $i_0 = 0$ and $F = F_2$. Solid curve—limit of existence of stochastic oscillations, calculated numerically for $i_0 = 0$ and $\beta = 50$. Dash-dot—limit obtained from Eq. (8) under the same conditions.

gions with and without the signal U (Ref. 9). The estimated maximum value of U , with allowance for the strong mismatch of the impedances of the junction and of the measuring amplifier, yields an equivalent noise temperature $T_n \sim 10^4$ K, which is close to the theoretical estimates.^{3,4}

Figure 5 shows the amplitude-frequency plane $[i_1, \omega]$ of the external-action parameters. The horizontal segments mark the frequency bands in which stochastic oscillations appear for the junctions listed in Table I. It can be seen that in the investigated junctions the stochastic oscillations occur in a wide range of variation of the normalized external-signal frequency, so that in practice these oscillations occur in the investigated frequency band in all junctions with high value of the parameter $\beta > 10$. The restrictions of the normalized frequencies, shown in Fig. 5, represent not vanishing of the stochastic oscillations, but limits of the experimental setup. The vertical lines show for junction No. 6 the initial sections where stochastic oscillations appear when the normalized amplitude of the microwave signal is varied at a fixed frequency. The normalized values of i_1 were determined from a comparison of the experimental and theoretical dependences of the critical current on the amplitude of the microwave current.

It can be seen from Fig. 5 that the experimental values i_1^{lim} of the limits of the regions where stochastic oscillations occur lie above the theoretical values obtained from Eq. (8). This relation between the analytical theory and experiment should be regarded as satisfactory, since Eq. (8) was derived under the condition of small perturbation and can serve as a lower bound of i_1^{lim} . A qualitative correspondence is also observed between the experimental data and the computer calculation, namely: the fact that $i_1^{\text{lim}}(\omega)$ has a minimum at $\omega \approx 0.8$ and that i_1^{lim} increases with increasing ω . For transitions with small $\beta < 15$ at $\omega > 1$ the bands in which the stochastic oscillations set in shrink into points. However, the observed minimum of i_1^{lim} is shifted towards larger ω , and the band in which the stochastic oscillations appear is substantially broader than that calculated. The deviation of the experiment from the numerical calculation is apparently due

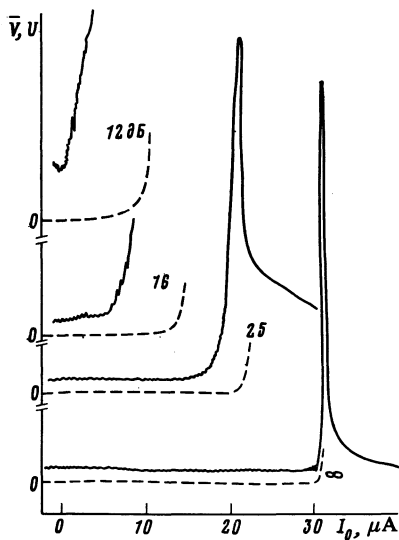


FIG. 6. Plots of $U(I_0)$ and initial sections of the CVC (dashed) at different damping levels for junction No. 6 with $\beta = 60$ and $\omega = 0.69$.

to the fact that the properties of a real junction differ strongly from those predicted by the resistive model, say because of the nonlinear voltage dependence of the junction quasiparticle current. We note that the discrepancy between the analytic theory and the calculation can be due to the fact that according to the analytic calculation the phase-space region in which the solutions of the system (2) behave in a complicated manner (see Fig. 1) is quite small (its measure is $\sim i_1 \ll 1$). If this region is not attracting,¹⁸ its presence is not revealed by the calculations. As a result, stochastic oscillations appear at large amplitudes of the external signal, $i_1 \sim 1$, when the validity of the derived Eq. (8) is not rigorously verified.

Figure 6 shows the dependences of the amplitude U at the frequency $F2$ on the dc current I_0 flowing through the junction at various applied microwave powers P , at a frequency $\omega = 0.69$ and at $\beta = 50$; also shown are the initial sections of the CVC. It can be seen that the presence of non-

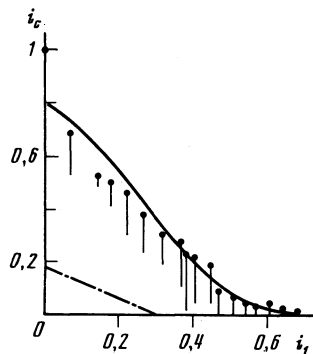


FIG. 7. Dependence of normalized critical current on the microwave current amplitude i_1 (points) in the region of appearance of stochastic oscillations in the presence of direct current through junction No. 6 with $\beta = 50$, $\omega = 0.69$ (vertical arrows). The solid curve is the numerically calculated $i_c(i_1)$ dependence, the dash-dot curve is the stochastic-oscillation existence limit obtained from (8).

zero I_0 gives rise to stochastic oscillations at lower values of i_1 . This "stimulation" of the stochastic oscillation by direct current agrees with the theoretical (8). Figure 7 shows the experimental dependence of the normalized critical current on the microwave amplitude i_1 . The solid line is the theoretical $i_c(i_1)$ dependence obtained with a computer within the framework of the resistive model. The vertical lines show the regions of the onset of the stochastic oscillations at a fixed value of i_1 . The dash-dot line is the stochastic-oscillation onset boundary calculated from Eq. (8). It can be seen that, just as at $i_0 = 0$, the boundary (8) passes below the experimental values. At the same time the numerically calculated boundary of the onset of stochastic oscillations coincides with the $i_c(i_1)$ dependence. It must be noted that for junctions with small values $\beta < 10$ deviations of the boundary of the region of the onset of the stochastic oscillations from that for junctions with large β were observed.¹⁹

4. CONCLUSION

The analytic expression obtained in this paper gives the lower bound of the experimentally observed limits of the onset of stochastic oscillations in Josephson tunnel junctions, and describes qualitatively the changes of these limits when the parameters β , ω , and i_0 are varied. Numerical calculations within the framework of the resistive model describe well a number of peculiarities experimentally observed in the junctions, such as the clearly pronounced minimum of the frequency dependence of the limiting signal amplitude $i_1^{\text{lim}}(\omega)$, the nonmonotonic dependence of the stochastic-oscillation level on the external signal amplitude, and others, although they yield larger values of i_1^{lim} than observed in experiment. The discrepancy between the calculation and experiment is probably due to failure to take into account the nonlinear voltage dependence of the quasiparticle current through the junctions, which is observable in real junctions, but which was not considered in the resistive model used in the calculations.

The authors thank Yu. D. Kalafati and V. K. Kornev for helpful discussions and E. B. Terent'ev for help with the numerical calculations.

¹⁾ By stable (unstable) manifold of a hyperbolic point of a mapping T is meant the geometric locus of the points that tend to the indicated point under the action of T^n as $n \rightarrow \infty$ (as $n \rightarrow -\infty$)

²⁾ The same condition as (8) for the onset of stochastic oscillations was obtained by Genchev *et al.* by another method.⁴

¹⁾ M. I. Rabinovich, *Usp. Fiz. Nauk* **125**, 123 (1978) [*Sov. Phys. Usp.* **21**, 443 (1978)].

²⁾ A. S. Pikovskii and M. I. Rabinovich, *Nelineinye volny (Nonlinear Waves)*, Nauka, 1979.

³⁾ B. A. Huberman, Y. P. Crutchfield, and N. H. Packard, *Appl. Phys. Lett.* **37**, 750 (1980).

⁴⁾ N. F. Pedersen and A. Davidson, *ibid.* **39**, 830 (1981).

⁵⁾ R. L. Kautz, *J. Appl. Phys.* **52**, 6241 (1981).

⁶⁾ M. Cirillo and N. F. Pedersen, *Phys. Lett.* **90A**, 150 (1982).

⁷⁾ E. Ben-Jacob, Y. Braiman, R. Shainsky, and Y. Imry, *Appl. Phys. Lett.* **38**, 822 (1981).

⁸⁾ V. K. Kornev and V. K. Semenov, *IEEE Trans. MAG-19*, 633 (1983).

⁹⁾ V. N. Gubankov, K. I. Konstaninyan, V. P. Koshelets, and G. A. Ovsyannikov, *Pisma v Zh. Tekh. Fiz.* **8**, 1332 (1982) [*Sov. J. Tech. Phys. Lett.* **8**, 574 (1982)].

- ¹⁰W. C. Stewart, *Appl. Phys. Lett.* **12**, 277 (1968). P. E. McCumber, *J. Appl. Phys.* **39**, 3113 (1968).
- ¹¹A. A. Andronov, A. A. Vitt, and S. E. Khaikin, *Theory of Oscillations*, Addison-Wesley, 1966.
- ¹²V. M. Alekseev, *Usp. Mat. Nauk* **36**, 161 (1981).
- ¹³V. K. Mel'nikov, *Trudy Mosk. Mat. Obshch-va* **12**, 1 (1963).
- ¹⁴Zh. D. Genchev, Z. G. Ivanov, and B. N. Todorov, *IEEE Trans. CAS-30*, No. 11 (1983).
- ¹⁵E. V. Astashkina and A. S. Mikhailov, *Zh. Eksp. Teor. Fiz.* **78**, 1636 (1980) [*Sov. Phys. JETP* **51**, 821 (1980)].
- ¹⁶A. N. Vystavkin, V. N. Gubankov, K. I. Konstantinyan, V. P. Koshelets, and Yu. V. Obukhov, *Zh. Tekh. Fiz.* **52**, 1637 (1982). [*Sov. Phys. Tech. Phys.* **27**, 1001 (1982)].
- ¹⁷R. F. Brook, R. Jaggi, R. B. Laibowitz, and T. O. Mohr, *Proc. LT-14*, **4**, 172 (1975).
- ¹⁸F. C. Moon and P. J. Holmes, *J. Sound Vibration* **65**, 275 (1979).
- ¹⁹V. N. Gubankov, K. I. Konstantinyan, V. P. Koshelets, and G. A. Ovsyannikov, *Trans. IEEE, MAG-19*, 637 (1983).

Translated by J. G. Adashko